Review of CMS contributions to Hadron Spectroscopy and planning forward

http://arxiv.org/abs/2204.06667

Snowmass Rare Processes and Precision Measurements Frontier Spring Meeting

University of Cincinnati

16-19 May, 2022

https://indico.fnal.gov/event/51844/

R. Chistov, V. Papadimitriou, S. Polikarpov, A. Pompili, A. Sanchez Hernandez

Outline

- Introduction
- Conventional Hadron Spectroscopy Results
- Exotic Hadron Spectroscopy Results
- New Decay Modes
- Perspectives
- Prospects for future running

Introduction

- CMS is providing significant contributions to hadron spectroscopy, especially to the beauty and quarkonium sectors, often utilizing final states containing muon pairs. This is possible due to:
  - Excellent tracking and muon identification performances
  - A flexible trigger system that is essential for increasing luminosities
  - Large production cross sections for heavy flavored particles

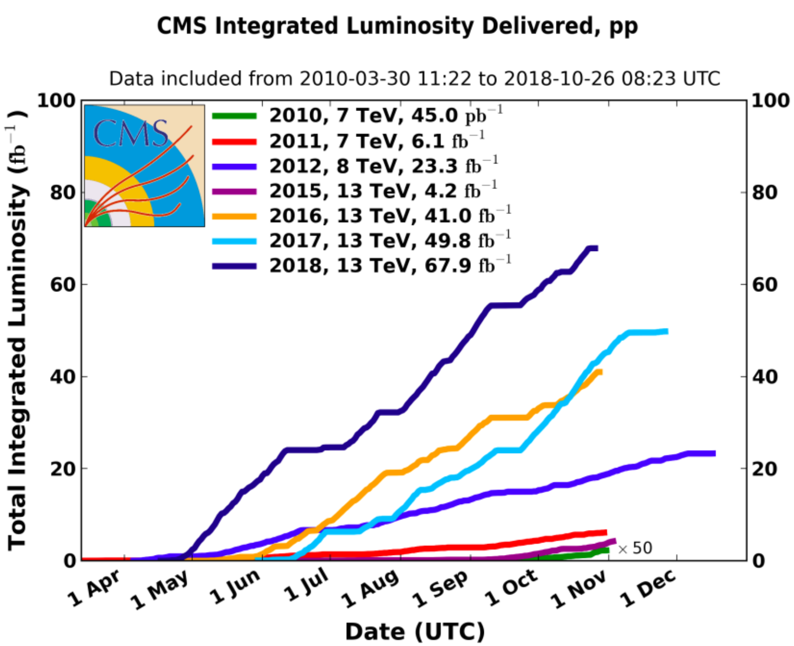

Data samples	$L_{\text{int}} \approx$
Run-I	
$\sqrt{s} = 7TeV$ 2011	**5**
$\sqrt{s} = 8TeV$ 2012	**20**
Run-II	
$\sqrt{s} = 13TeV$ 2015	**4**
2016	**38**
2017	**45**
2018	**60**

LHC Schedule as of January 2022

Longer term LHC schedule

In January 2022, the schedule was updated with long shutdown 3 (LS3) to start in 2026 and to last for 3 years.

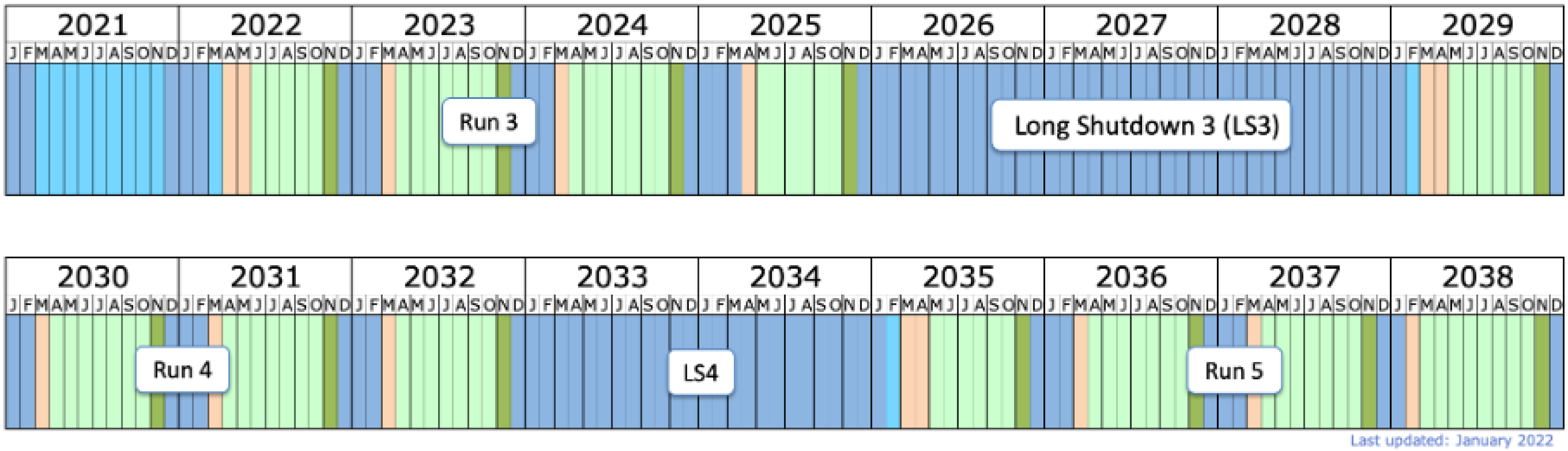

HL-LHC era

https://lhc-commissioning.web.cern.ch/schedule/LHC-long-term.htm

- The CMS Phase-1 Detector Upgrade will be operational during Run 3, starting this summer
- The CMS Phase-2 Detector Upgrade will be operational during the HL-LHC era

CMS Phase-II Upgrade (overview)

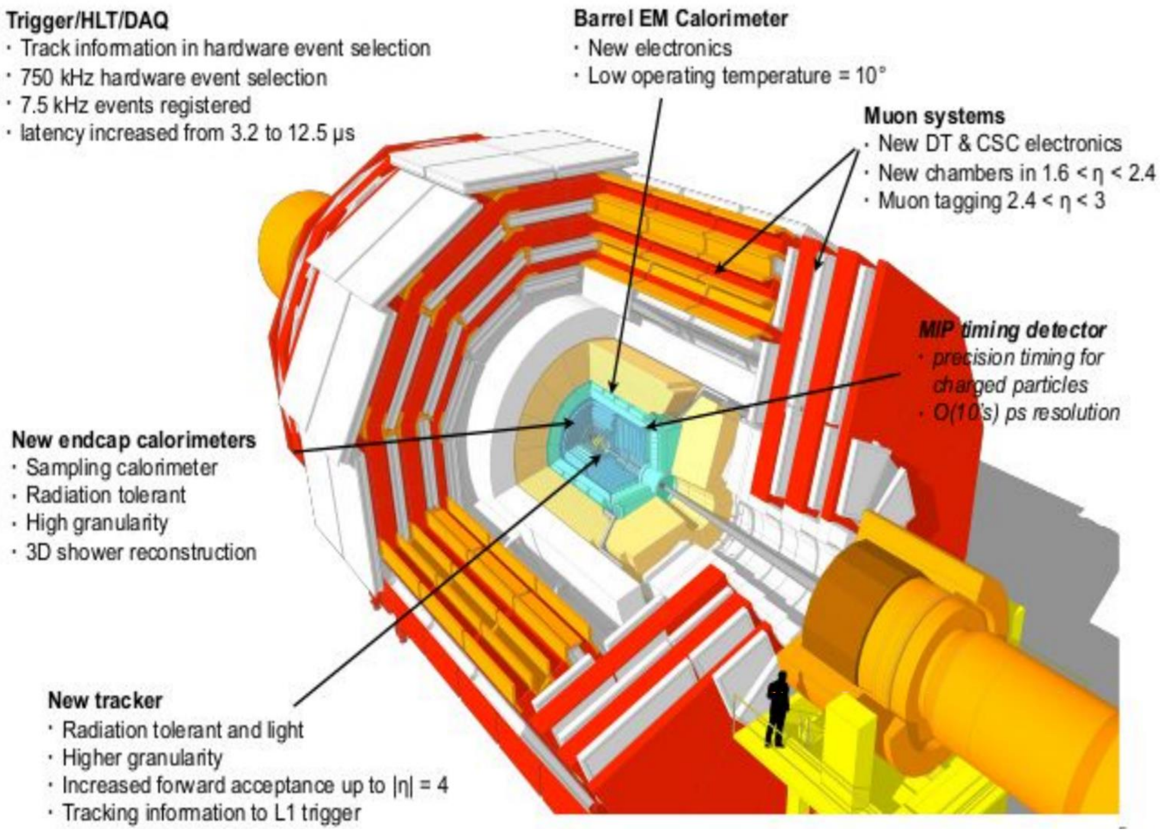

- A new tracker with improved p_T resolution and radiation hardness, lower material budget, extended coverage
- increased muon coverage
- a new forward calorimeter with high granularity and resolution
- addition of the MIP timing detector (MTD)
- increased trigger bandwidth & latencies
- inclusion of tracking information at L1 trigger
- replacement of electronics

- Conventional Hadron Spectroscopy Results

Observation of radially excited B_c^+ mesons

- CMS observed for the first time the two radially excited states $B_c^+(2S)$ and $B_c^{*+}(2S)$ decaying to $B_c^{+(*)}\pi^+\pi^-$.
  - Undetected very soft photon $B_c^{*+}(2S) \to B_c^{*+}\pi^+\pi^-, B_c^{*+} \to B_c^+\gamma$
  - Mass resolution agrees with MC expectations (~6MeV)
  - Local significance exceeding 6.5σ for observing two peaks rather than one. For both single peaks, significance > 5σ.

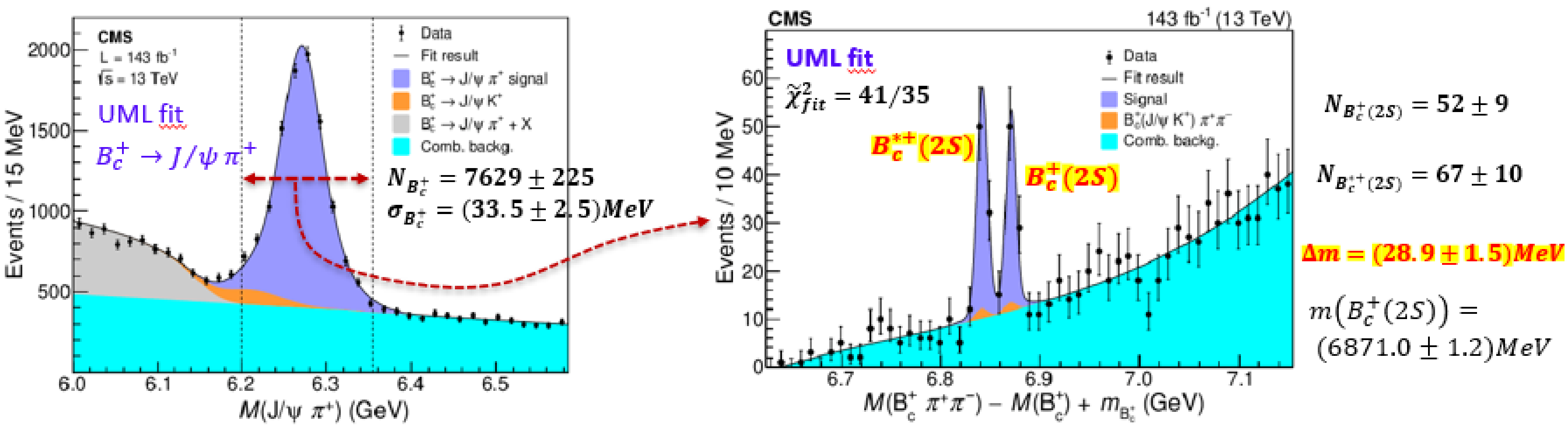

PRL 122 (2019) 132001

Differential production cross section ratios

PRD, 102 (2020) 092007

$$R^{+} \equiv \frac{\sigma(B_c(2S)^+)}{\sigma(B_c^+)} \mathcal{B}(B_c(2S)^+ \to B_c^+\pi^+\pi^-) = \frac{N(B_c(2S)^+)}{N(B_c^+)} \frac{\epsilon(B_c^+)}{\epsilon(B_c(2S)^+)},$$

$$R^{*+} \equiv \frac{\sigma(B_c^*(2S)^+)}{\sigma(B_c^+)} \mathcal{B}(B_c^*(2S)^+ \to B_c^{*+}\pi^+\pi^-) = \frac{N(B_c^*(2S)^+)}{N(B_c^+)} \frac{\epsilon(B_c^+)}{\epsilon(B_c^*(2S)^+)},$$

$$R^{*+}/R^{+} = \frac{\sigma(B_c^*(2S)^+)}{\sigma(B_c(2S)^+)} \frac{\mathcal{B}(B_c^*(2S)^+ \to B_c^{*+}\pi^+\pi^-)}{\mathcal{B}(B_c(2S)^+ \to B_c^+\pi^+\pi^-)} = \frac{N(B_c^*(2S)^+)}{N(B_c(2S)^+)} \frac{\epsilon(B_c(2S)^+)}{\epsilon(B_c^*(2S)^+)}.$$

$$R^{+} = (3.47 \pm 0.63\,(\text{stat}) \pm 0.33\,(\text{syst}))\%,$$
$$R^{*+} = (4.69 \pm 0.71\,(\text{stat}) \pm 0.56\,(\text{syst}))\%,$$
$$R^{*+}/R^{+} = 1.35 \pm 0.32\,(\text{stat}) \pm 0.09\,(\text{syst}).$$

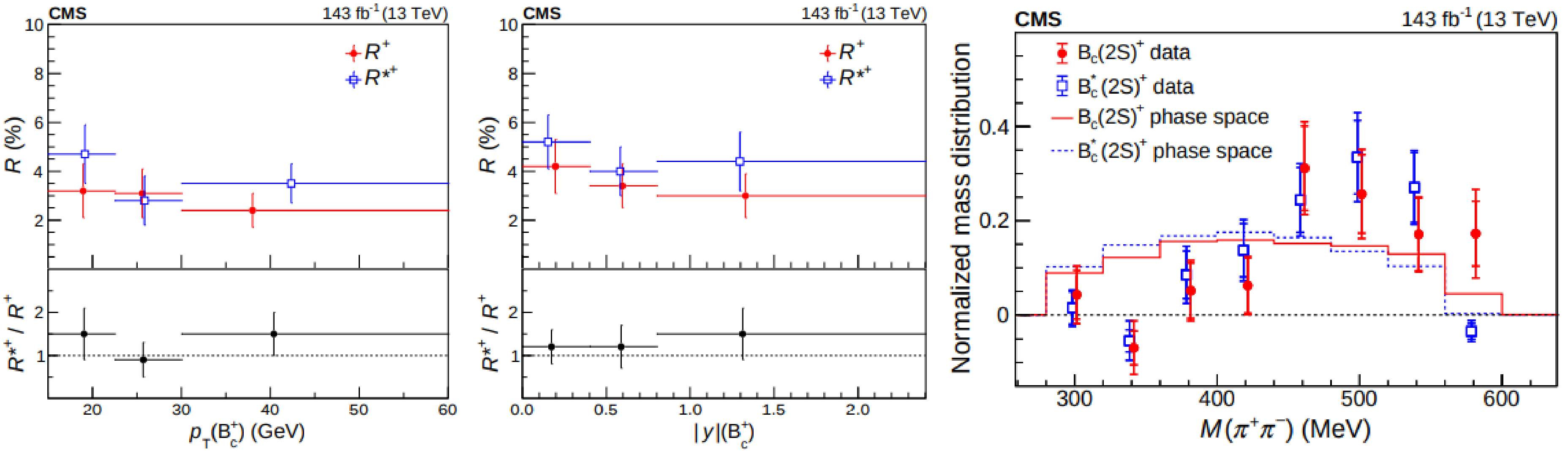

- No significant dependence of the three cross section ratios on $p_T(B_c^+)$ and $|y|(B_c^+)$
- In the normalized di-pion invariant mass observed different shapes from phase space but not fully significant with the available statistics.

First observation of resolved $\chi_{bj}(3P)$ states

- $\chi_{bj}(3P)$ is particularly interesting since its properties could have been affected by the nearby $B\overline{B}^{(*)}$ thresholds.
  - Radiative decays to $\Upsilon(3S)\gamma$
  - Low energy photons detected after conversion to e^+e^- pairs; $\chi_{bj}(3P)$ mass resolution of $\mathbf{2.18 \pm 0.32}\,\boldsymbol{MeV}$
  - Total (2-peak) yield: $\mathbf{372 \pm 36}$
  - 2-peak local stat. significance >9σ

PRL 121 (2018) 092002

$$M[\chi_{b1}(3P)] = (10513.42 \pm 0.41 \pm 0.18)\,\text{MeV},$$

$$M[\chi_{b2}(3P)] = (10524.02 \pm 0.57 \pm 0.18)\,\text{MeV},$$

$$\Delta m_{21} \equiv m(\chi_{b2}) - m(\chi_{b1}) = (10.6 \pm 0.64 \pm 0.17)\,\text{MeV}.$$

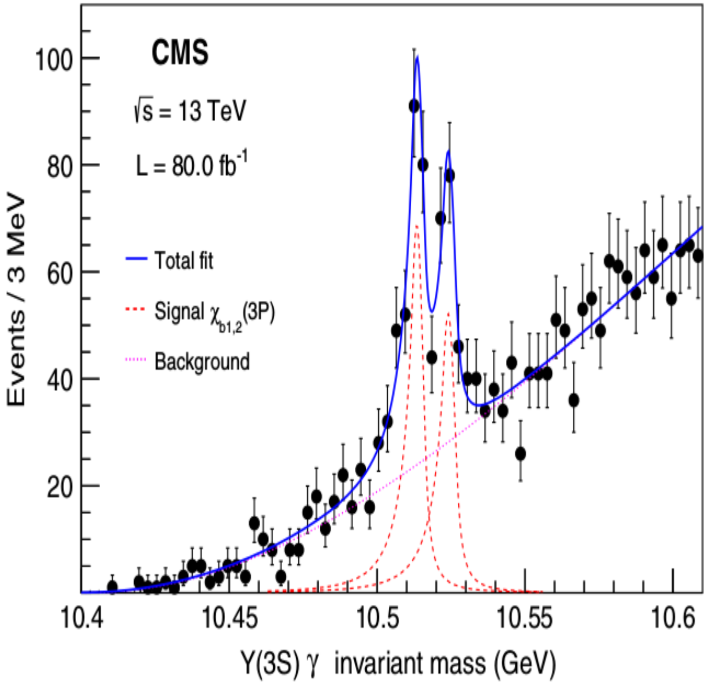

The measurement supports the standard hierarchy (J=2 heavier than J=1)

First observation of resolved $\chi_{bj}(3P)$ states

- This measurement fills the gap in the spin-dependent bottomonium spectrum below the open beauty threshold.
- It also contributes to the understanding of non-perturbative spin-orbit interaction affecting quarkonium spectroscopy.
- No CMS observation so far of the $\chi_{b0}(3P)$ radiative decay.

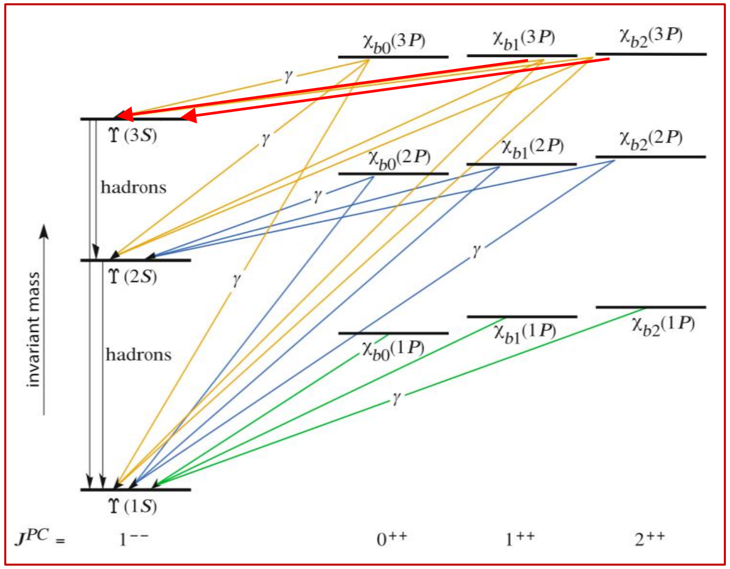

TABLE II. Mass splitting (in MeV) of 3P-wave bottomonia in our UQM [12], Godfrey-Isgur (GI) model [16], modified GI model [17], and constituent quark model (CQM) [18]. The later three models are regarded as quenched quark models.

Mass splitting	Our UQM [12]	GI [16]	Modified GI [17]	CQM [18]	Experiment [1]
$\chi_{b1}(3P) - \chi_{b0}(3P)$	23	16	14	13	...
$\chi_{b2}(3P) - \chi_{b1}(3P)$	12	12	12	9	$(10.6 \pm 0.64 \pm 0.17)$

From: M. Anwar et al., PRD99 (2019) 094005

Λ_b^0 excited states in low-mass region

- Confirmation of $\Lambda_b(5912)^0$ and first confirmation of $\Lambda_b(5920)^0$
  - Use $\Lambda_b^0 \to J/\psi\, \Lambda$ & $\Lambda_b^0 \to \psi(2S)\Lambda$ [with $\psi(2S) \to \mu\mu, J/\psi\, \pi\pi$] by triggering on dimuons

$$M(\Lambda_b(5912)^0) = [5912.32 \pm 0.12(stat) \pm 0.01(syst) \pm 0.17(m_{PDG}(\Lambda_b^0))]\text{MeV}$$

$$M(\Lambda_b(5920)^0) = [5920.16 \pm 0.07(stat) \pm 0.01(syst) \pm 0.17(m_{PDG}(\Lambda_b^0))]\text{MeV}$$

PLB 803 (2020) 135345

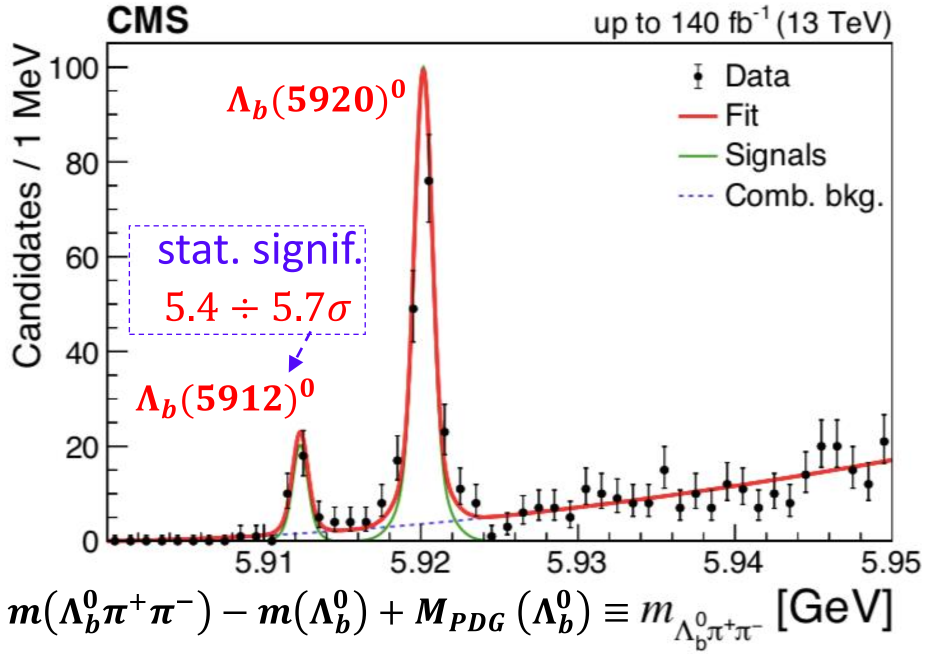

Λ_b^0 excited states in high-mass region

- First confirmation of $\boldsymbol{\Lambda_b(6146)^0}$ and $\boldsymbol{\Lambda_b(6152)^0}$
  - One-peak hypothesis vs BKG-only has significance > 5.4 – 6.5σ

$$M(\Lambda_b(6146)^0) = [6146.5 \pm 1.9(stat) \pm 0.8(syst) \pm 0.2(m_{PDG}(\Lambda_b^0))]\text{MeV}$$

$$M(\Lambda_b(6152)^0) = [6152.7 \pm 1.1(stat) \pm 0.4(syst) \pm 0.2(m_{PDG}(\Lambda_b^0))]\text{MeV}$$

PLB 803 (2020) 135345

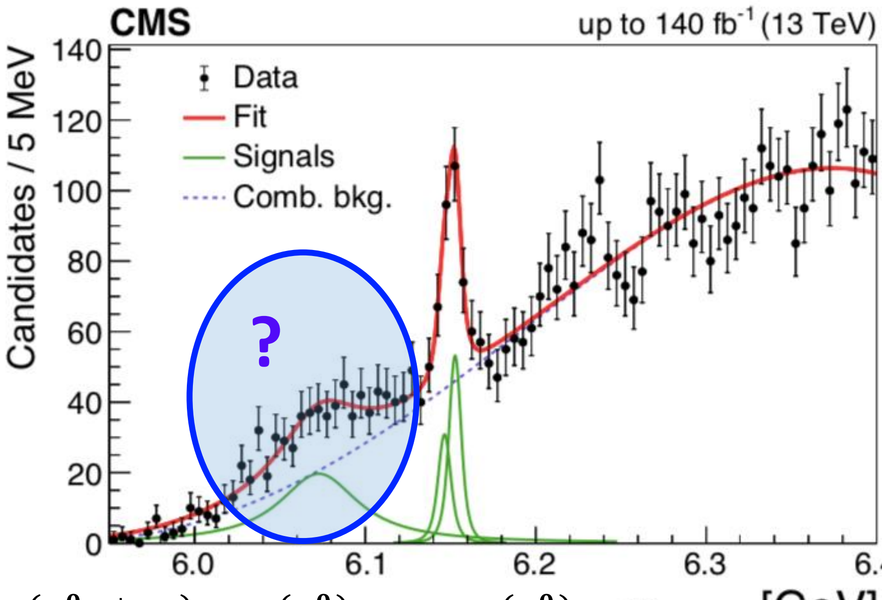

$\boldsymbol{m(\Lambda_b^0\pi^+\pi^-) - m(\Lambda_b^0) + M_{PDG}(\Lambda_b^0)} \equiv m_{\Lambda_b^0\pi^+\pi^-}$ [GeV]

Assuming a single broad resonance X_b the fit with M and Γ as free parameters provides (with stat. sign. of ~ 4σ):

$$M(X_b) = [6073 \pm 5(stat)]MeV$$

$$\Gamma(X_b) = [55 \pm 11(stat)]MeV$$

Confirmed by LHCb as a further excited state: $\boldsymbol{\Lambda_b(6072)^{**0}}$

Observation of new beauty- strange baryons

- Using the 2011 data, CMS observed a new **Ξ baryon** (Ξ_b^{*0}) via its strong decay to $\Xi_b^{\mp}\pi^{\pm}$. The Ξ_b was reconstructed via: $\Xi_b^- \rightarrow J/\psi\, \Xi^-$
  - significance > 5 σ

PRL 108 (2012) 252002

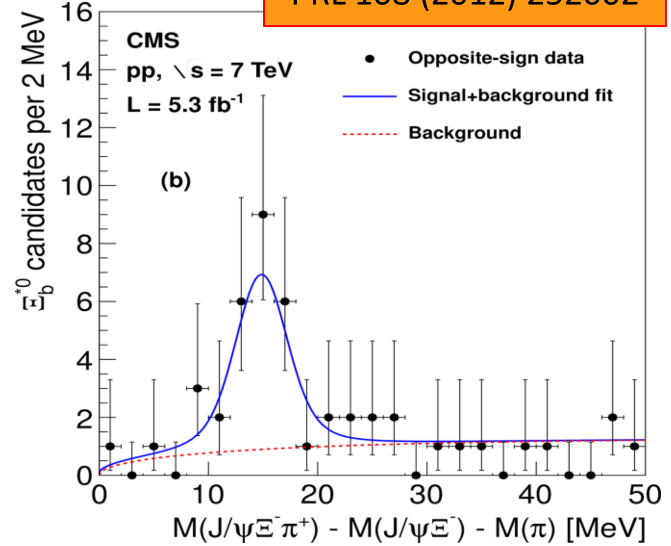

- Recently CMS observed: $\Xi_b^{**}(6100)^- \rightarrow \Xi_b^-\pi^+\pi^-$, including the intermediate resonance $\Xi_b^{*0} \rightarrow \Xi_b^-\pi^+$

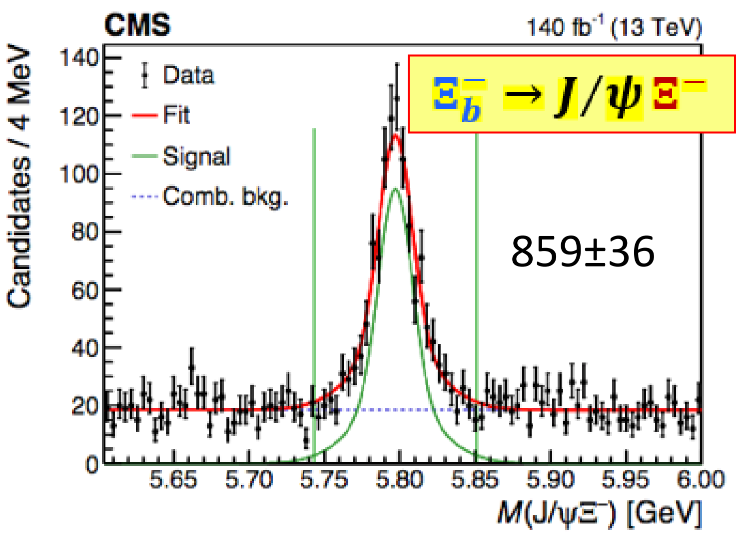

$\Xi_b^- \rightarrow J/\psi\, \Xi^-$

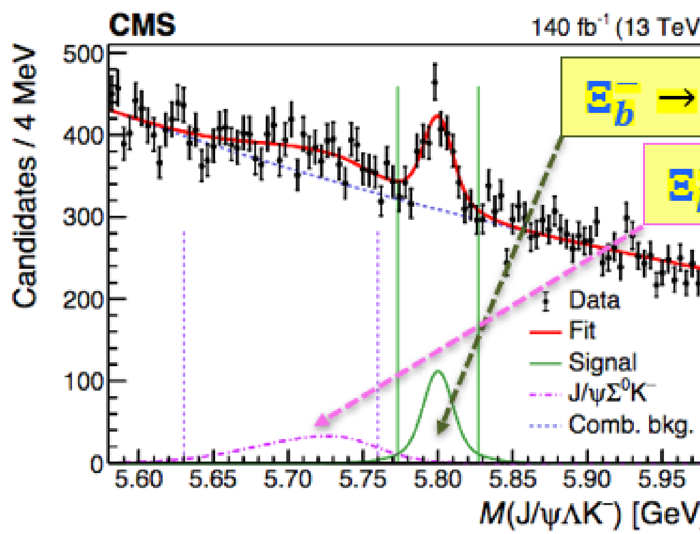

$\Xi_b^- \rightarrow J/\psi\, \Lambda^0 K^-$

$\Xi_b^- \rightarrow J/\psi\, \Sigma^0 K^-$

(partially reconstructed: $\Sigma^0 \rightarrow \Lambda^0\gamma$ where the soft γ is undetected)

Observation of the excited beauty strange baryon $\Xi_b^{**}(6100)^-$

PRL 126 (2021) 252003

- The invariant mass of the final state is built by combining the fully reconstructed decays (left) with the partially reconstructed channel (right) - 30% higher mass resolution.

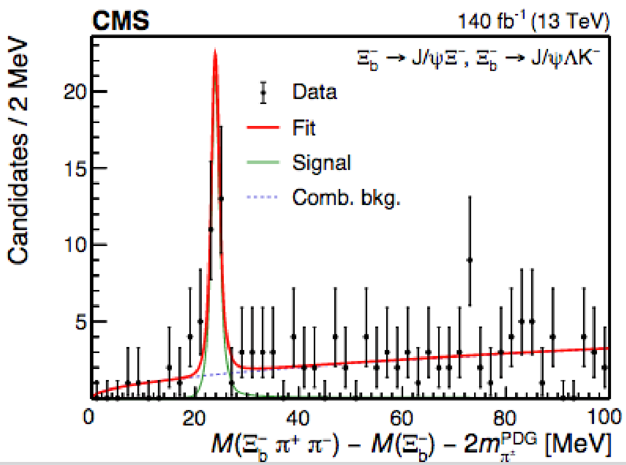

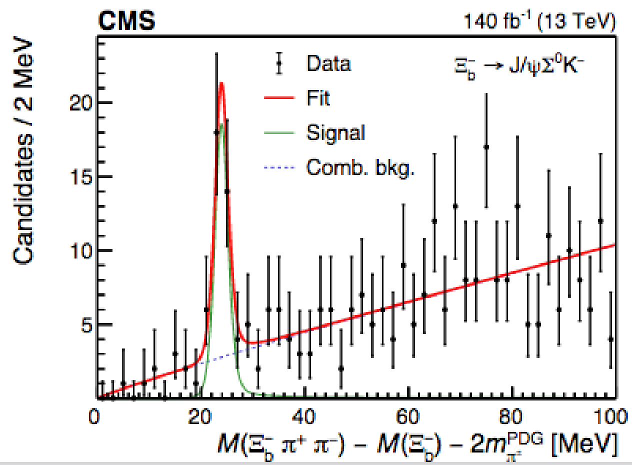

(local stat. signif. ~6.2-6.7σ)

$m(\Xi_b^{**-}) = [\,6100.3$

$\pm 0.2(\text{stat}) \pm 0.1(\text{sys})$

$\pm 0.6(\Xi_b^-)\,]$ MeV

$\Gamma(\Xi_b^{**-}) < 1.9\text{MeV}$ @95%CL

The low yield does not allow a measurement of the quantum numbers. However following analogies with the established Ξ_c baryon states …

… the new $\Xi_b^{**}(6100)^-$ resonance is the analogue **of Ξ_c(2815)** and its decay sequence is consistent with the lightest orbitally excited Ξ_b^- baryon with $J^P = 3/2^-$[L=1 between b-quark and (ds)-diquark]

- Exotic Hadron Spectroscopy Results

X(3872) in pp collisions

JHEP 04 (2013) 154

- As soon as LHC started, CMS confirmed the X(3872) state inclusively and exclusively reconstructing it in the J/ψππ final state.

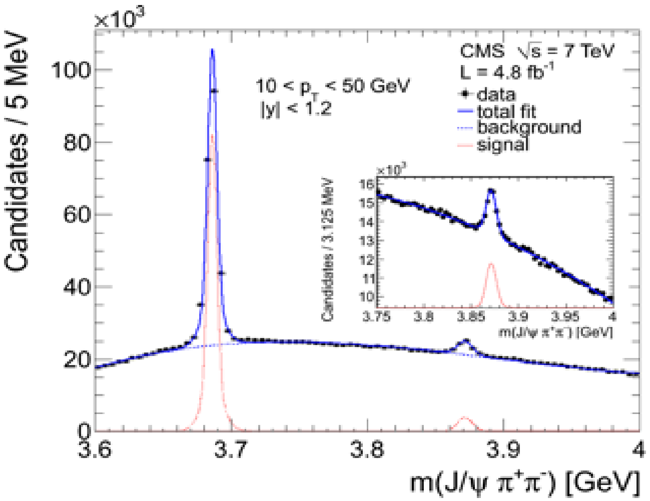

Compact multiquark?
Loosely bound hadronic molecule?
Mixture of charmonium and S-wave molecule?
…………….

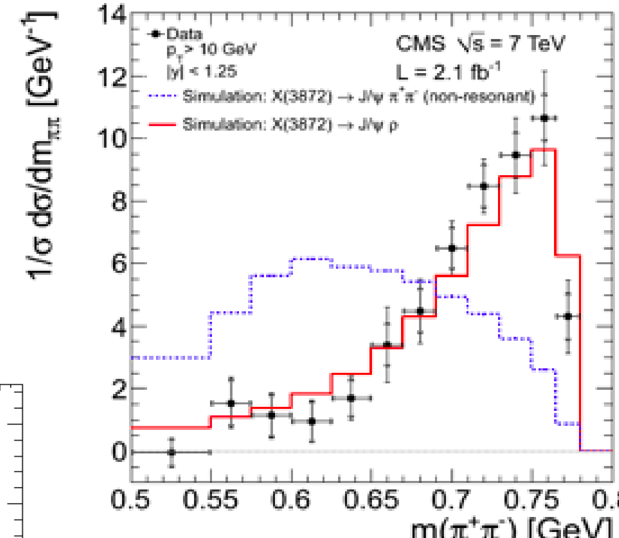

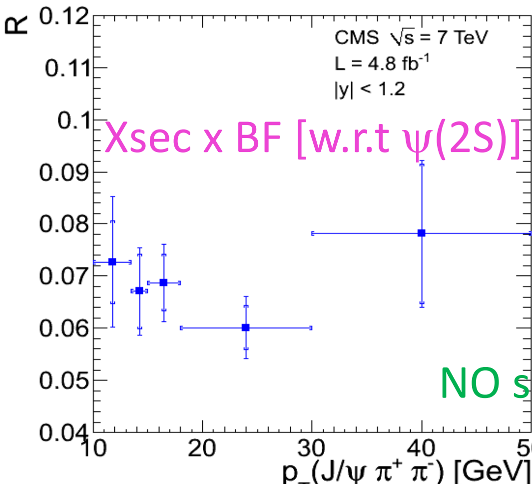

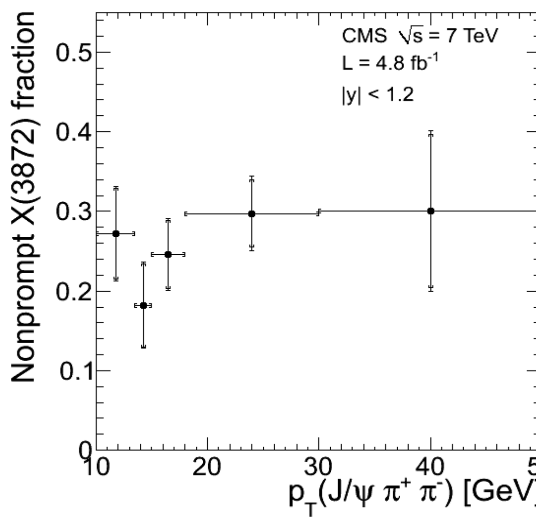

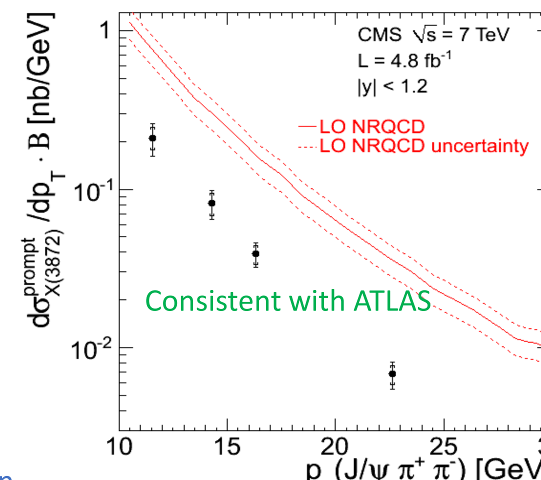

NO significant dependance on p_T

First evidence of X(3872) in PbPb collisions

PRL 128 (2022) 032001

- The study of X(3872) production rate in HI collisions, with reference to a standard charmonium (ψ(2S)), may help to separate a compact tetraquark configuration (radius ~*1fm*) from a large-sized configuration of a molecular state (radius ~*10fm*).

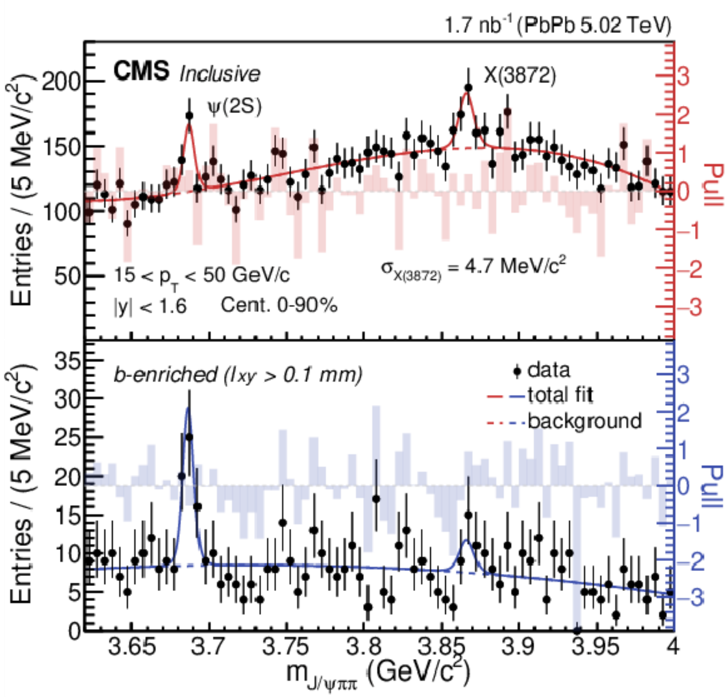

Stat. significance ~ 4.2 σ

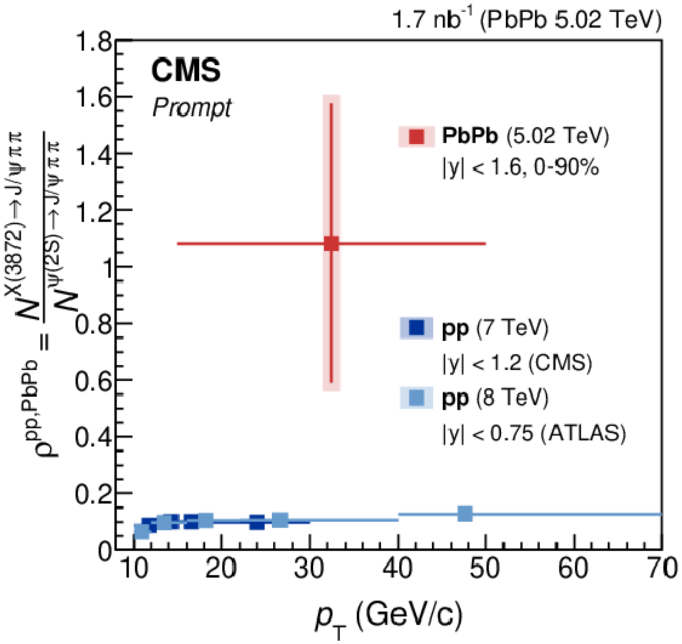

More statistics and improved systematics needed.

$\boldsymbol{R(PbPb)} = 1.08 \pm 0.49(stat.) \pm 0.52(syst.)$

$\boldsymbol{R(pp)} \sim 0.1$ (both ATLAS & CMS)

Observation of new decay mode $B_s^0 \to X(3872)\phi$

PRL 125 (2020) 152001

- The signal of $\boldsymbol{B_s^0 \to X(3872)\phi}$ is extracted with reference to the control channel $\boldsymbol{B_s^0 \to \psi(2S)\phi}$ which is used as normalization for the BF measurement as many systematics cancel in the ratio.

- Signal yield determined from a simultaneous 2D fit of the distributions: $\boldsymbol{m(J/\psi\,\pi^+\pi^-)}$, $\boldsymbol{m(K^+K^-)}$

$$N(B_s^0 \to X(3872)\phi) = 299 \pm 39$$

significance > 6σ

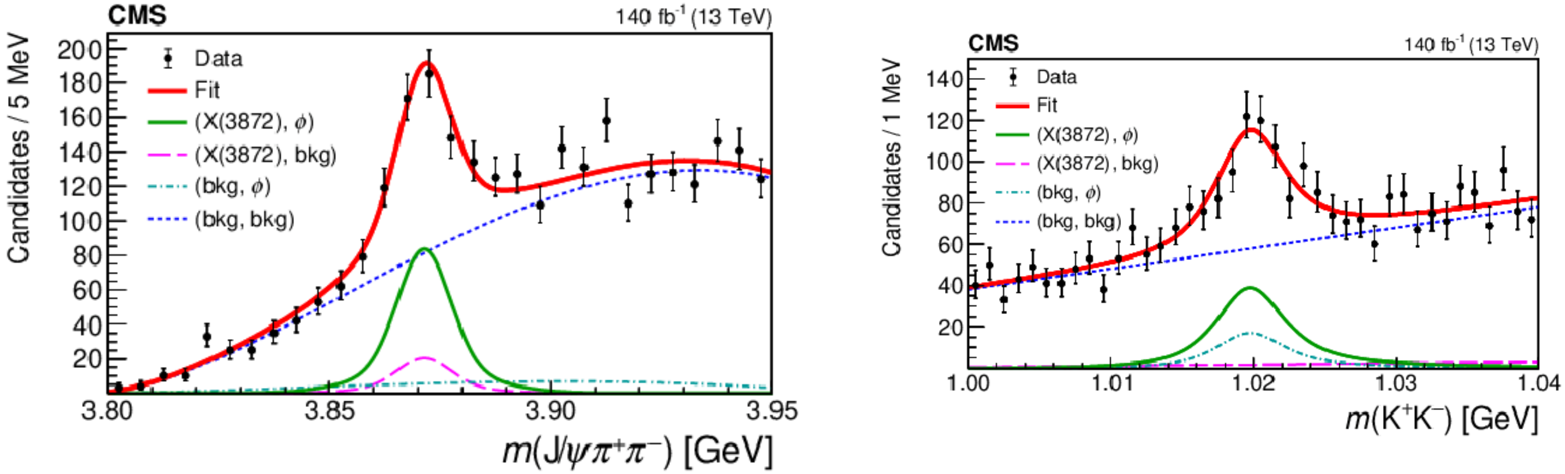

Product of branching fractions for $B_s^0 \to X(3872)\phi$ measured relative to $B_s^0 \to \psi(2S)\phi$:

$$\frac{\mathcal{B}(B_s^0 \to X(3872)\phi)}{\mathcal{B}(B_s^0 \to \psi(2S)\phi)} \times \frac{\mathcal{B}(X(3872) \to J/\psi\pi^+\pi^-)}{\mathcal{B}(\psi(2S) \to J/\psi\pi^+\pi^-)} = (2.21 \pm 0.29(\text{stat}) \pm 0.17(\text{syst}))\%$$

Observation of new decay mode $B_s^0 \to X(3872)\phi$

- Branching fraction consistent with that of the $B^0 \to X(3872)K^{(*)0}$

$$\mathcal{B}(B_s^0 \to X(3872)\phi)\mathcal{B}(X(3872) \to J/\psi\pi^+\pi^-) = (4.14 \pm 0.54(\text{stat}) \pm 0.32(\text{syst}) \pm 0.46(\mathcal{B}))\times 10^{-6}$$

$$\mathcal{B}(B^0 \to X(3872)K^0)\mathcal{B}(X(3872) \to J/\psi\pi^+\pi^-) = (4.3 \pm 1.3)\times 10^{-6}$$

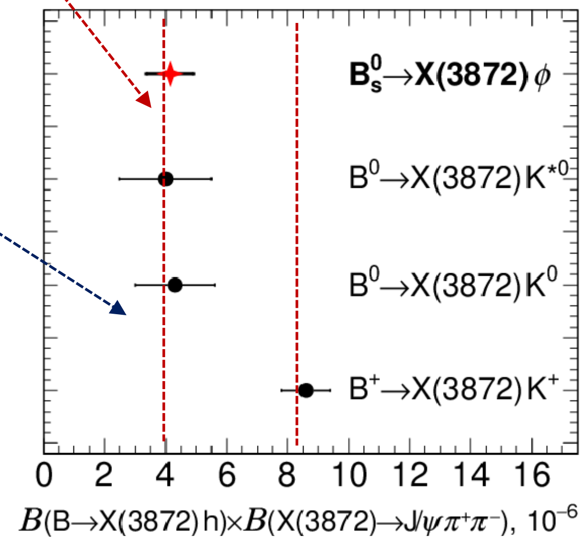

- Significant difference in BF ratio (B_s^0 to B^+ compared to the $\psi(2S)$ modes):

$$\frac{\mathcal{B}(B_s^0 \to X(3872)\phi)}{\mathcal{B}(B^+ \to X(3872)K^+)} = 0.482 \pm 0.063(\text{stat}) \pm 0.037(\text{syst}) \pm 0.070(\mathcal{B})$$

$$\frac{\mathcal{B}(B_s^0 \to \psi(2S)\phi)}{\mathcal{B}(B^+ \to \psi(2S)K^+)} = 0.87 \pm 0.10$$

- This suggests a difference in the production dynamics of the exotic X(3872) state in B^0 and B_s^0 decays compared to B^+ with respect to the standard $\psi(2S)$.

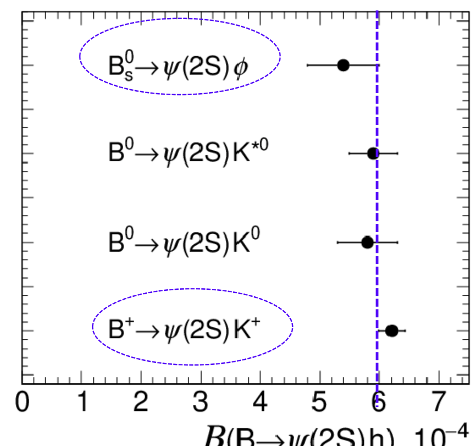

Search for X_b, the bottomonium counterpart of X(3872)

PLB 727 (2013) 57

- Looked for the $X_b \to \Upsilon(1S)\,\pi^+\pi^-$ decay, analogous to $X(3872) \to J/\psi\ \pi^+\pi^-$
- The Molecular Model suggests to search close to the $B\bar{B}^{(*)}$ threshold of 10.562 GeV

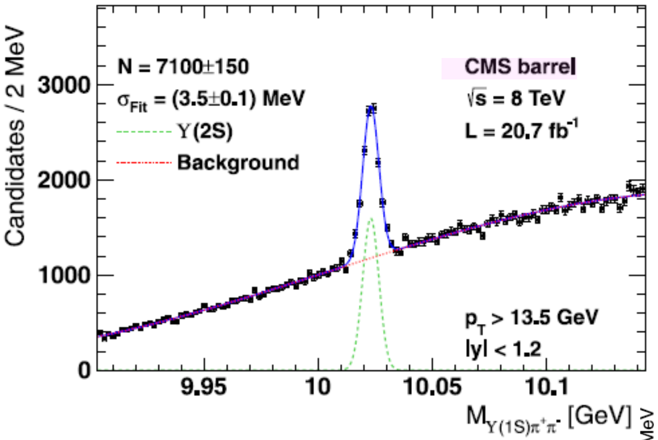

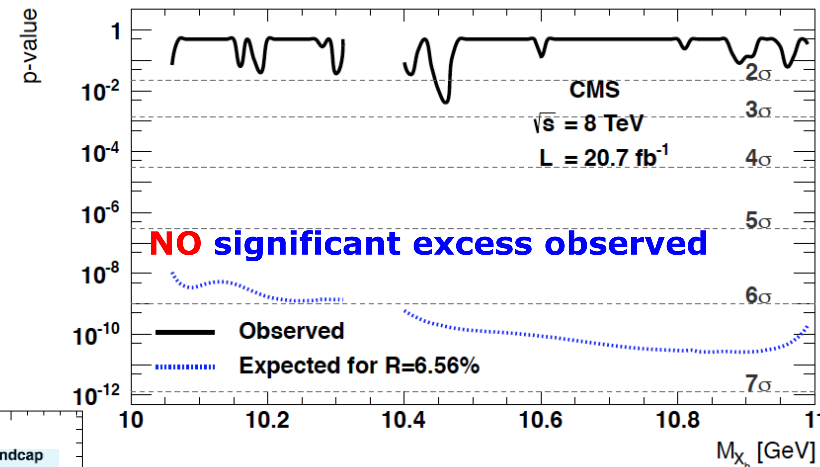

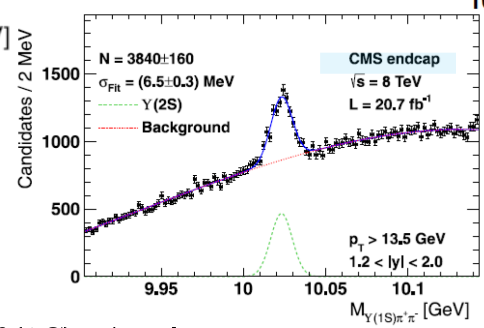

$$R \equiv \frac{\sigma(pp \to X_b)}{\sigma(pp \to \Upsilon(2S))} \cdot \frac{BF(X_b \to \Upsilon(1S)\pi^+\pi^-)}{BF(\Upsilon(2S) \to \Upsilon(1S)\pi^+\pi^-)}$$

95% CL upper limit set on the ratio *R* :

observed UL range: 0.9% to 5.4%

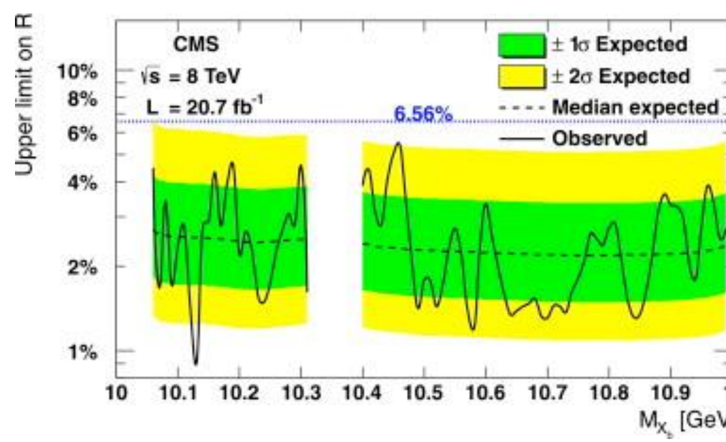

Similar result from ATLAS

Search for a $bb\bar{b}\bar{b}$ tetraquark state

PLB 808 (2020) 135578

- Recent theoretical predictions of tetraquarks consisting of two beauty quarks and two antiquarks and having mass of about 2 x M(Υ(1S)) or 2 x M(η_b), that is in the 18-19 GeV range.
- No significant narrow excess of candidates observed above the background expectation in the Υ(1S)$\mu^+\mu^-$ final state.
- Upper limits on the product of the production cross section of a resonance & the BF to the final state of 4 muons via an intermediate Υ(1S) are set @95% CL.

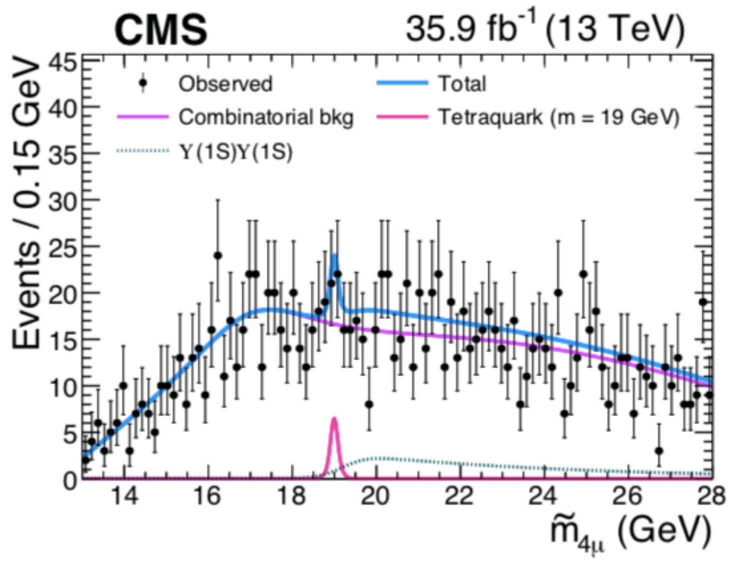

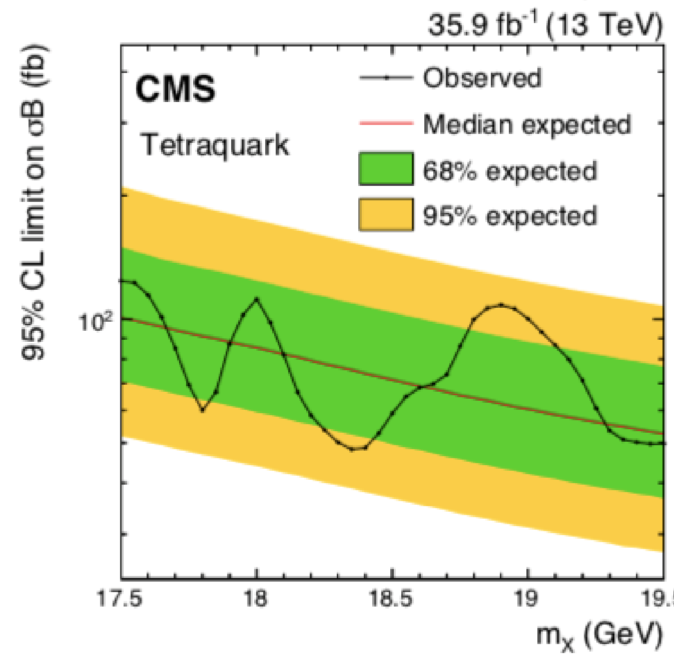

- New b hadron decay modes studied

New Decay Modes

arXiv:2201.09131
EPJC accepted

- Observation of the $B^0 \to \psi(2S)K^0_S\pi^+\pi^-$ and $B^0_s \to \psi(2S)K^0_S$ decays.

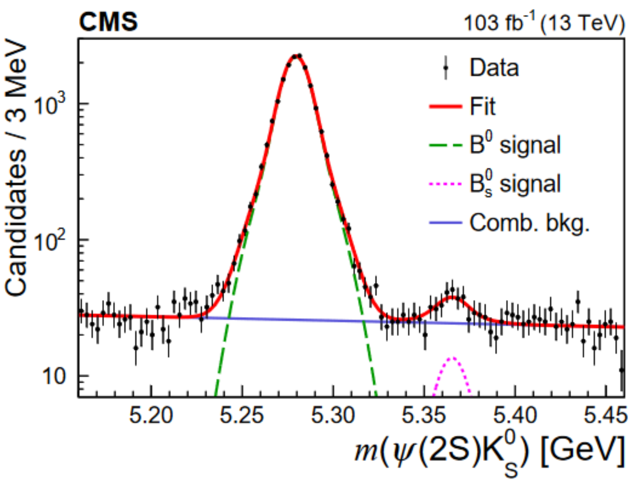

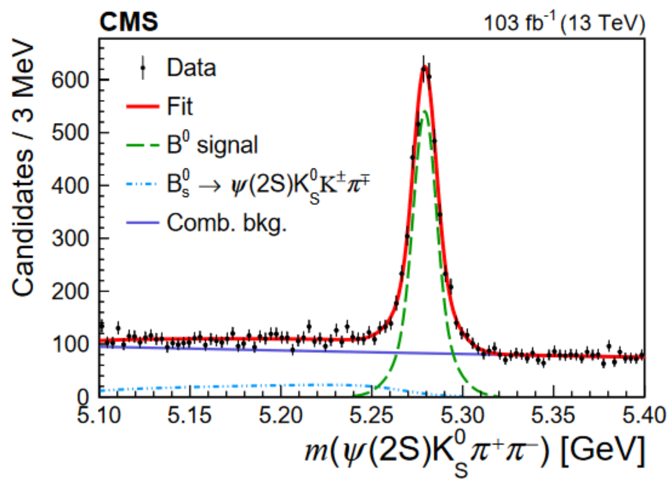

Resulting BFs measured for first time

$\mathcal{B}(B_s^0 \to \psi(2S)K_S^0)/\mathcal{B}(B0 \to \psi(2S)K_S^0) = (3.33 \pm 0.69\text{ (stat)} \pm 0.11\text{ (syst)} \pm 0.34\text{ (fs / fd)}) \times 10^{-2}$

$\mathcal{B}(B^0 \to \psi(2S)K_S^0\pi^+\pi^-)/\mathcal{B}(B^0 \to \psi(2S)K_S^0) = 0.480 \pm 0.013\text{ (stat)} \pm 0.032\text{ (syst)}$

- Observation of the $\Lambda_b^0 \to J/\psi\Lambda\phi$ decay. (13 TeV, 60 fb^{-1})

$\mathcal{B}(\Lambda_b^0 \to J/\psi\Lambda\phi)/\mathcal{B}(\Lambda_b^0 \to \psi(2S)\Lambda) = (8.26 \pm 0.90\text{ (stat)} \pm 0.68\text{ (syst)} \pm 0.11(\mathcal{B}))\times 10^{-2}$

PLB 802 (2020) 135203

New Decay Modes

EPJC (2018) 78:939

- Observation of the decay mode $B^*_{s2}(5840)^0 \rightarrow B^0 K^0_S$ and measurement of its BF relative to $B^*_{s2}(5840)^0 \rightarrow B^+ K^-$.

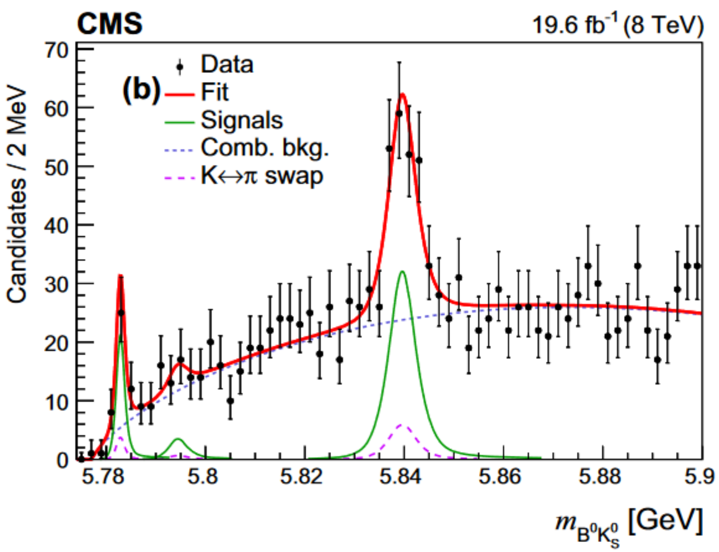

$$R_2^{0\pm} = \frac{\mathcal{B}(B^*_{s2} \rightarrow B^0 K^0_S)}{\mathcal{B}(B^*_{s2} \rightarrow B^+ K^-)} = 0.432 \pm 0.077 \pm 0.075 \pm 0.021$$

$$\Gamma_{B^*_{s2}} = 1.52 \pm 0.34 \pm 0.30\,\mathrm{MeV}$$

- Observation of the decay mode

$B^+ \rightarrow \psi(2S)\phi(1020)K^+$

$\mathcal{B}(B^+ \rightarrow \psi(2S)\phi K^+) =$

$(4.0 \pm 0.4\,(\mathrm{stat}) \pm 0.6\,(\mathrm{syst}) \pm 0.2\,(\mathcal{B})) \times 10^{-6}$

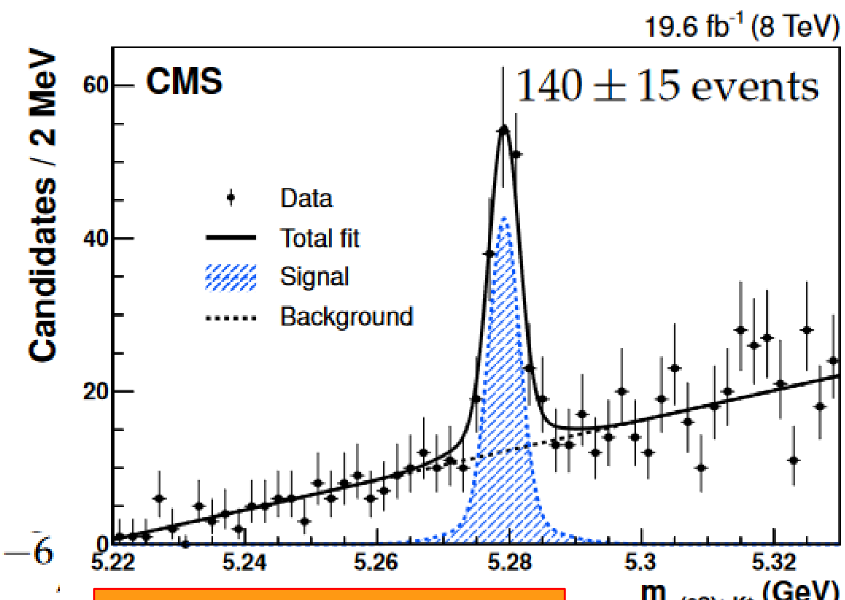

PLB 764 (2017) 66

- Perspectives and Prospects

Detector, Trigger and Reconstruction strengths

- Particular strengths of the CMS detector and reconstruction algorithms for this type of physics are:
  - The **large muon acceptance,** especially useful for the extraction of **bottomonium** signals and in general for all **double quarkonia**.
  - The ability to use effectively **photon conversions** for the precise measurement of radiative spectroscopic transitions (E_γ>400MeV) when resolution is important. For rare processes calorimeter photons can be exploited as well.
  - The **good efficiency for the low momentum tracks**, both prompt and displaced from the Primary Vertex.

Displaced tracks are crucial for the reconstruction of the $K_S^0 \to \pi^+\pi^-$, $\Lambda^0 \to p\pi^-$ and $\Xi^- \to \Lambda^0\pi^-$ decays.

For example, the π^- from the $\Xi^- \to \Lambda^0\pi^-$ decays are **very soft** and **displaced** !

Decay chain from $\Xi_b^{**}(6100)^- \to \Xi_b^-\pi^+\pi^-$

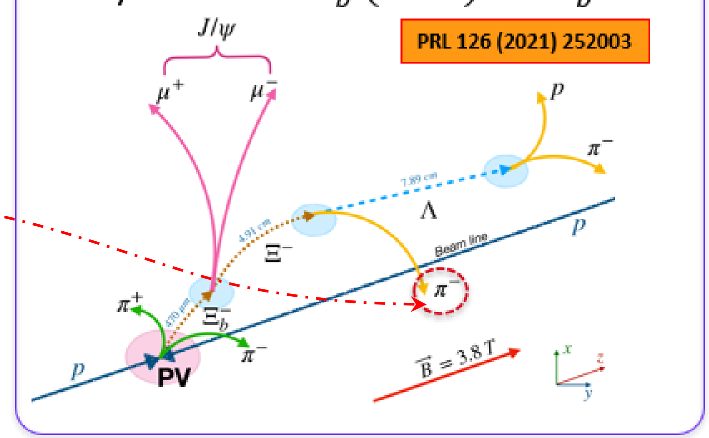

Detector, Trigger and Reconstruction Strengths

- The B-physics parking campaign has recorded ~$\mathbf{10^{10}}$ ***unbiased* decays of beauty hadron** during the 2018 Run, **exploiting the flexibility of CMS data taking model (**as luminosity drops in the fill the L1 rate is kept ~constant & the HLT rate increased towards the end of each fill). **Trigger/tag-side requires a muon coming from a displaced vertex.** Completed reconstruction of these 12B events at the end of 2019 [http://cds.cern.ch/record/2704495] and we have on tape:

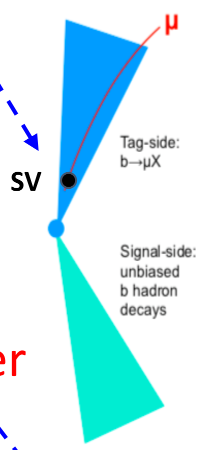

- **B-parked data set opens several prospects for spectroscopy studies**; its potentiality is still being studied.
- The possibility to continue B-parking efforts in Run-3 is currently under consideration.
- Further spectroscopy in charm sector can be carried out utilizing semileptonic decays; charmed hadrons can be produced :
  - either at *tag side* ($b \to \boldsymbol{c}\,\boldsymbol{\mu}\,\nu$)
  - and at *probe side* (when $\boldsymbol{c} \to s\,\boldsymbol{\mu}\,\nu$ at *tag side*)

Mode	N_{2018}	f_B
	Generic b hadrons	
B^0_d	4.0×10^9	0.4
$B^\pm$	4.0×10^9	0.4
B_s	1.2×10^9	0.1
b baryons	1.2×10^9	0.1
B_c	1.0×10^7	0.001
Total	1.0×10^{10}	1.0

Detector, Trigger and Reconstruction Strengths

- "Standard" triggers will record large amounts of well-reconstructed b-hadrons in charmonium decay modes, as well as charmonium and bottomonium states.
  - Smart compromise between available trigger rate and kinematic threshold under investigation for Run-3 and beyond
  - High Level Trigger (HLT) budget rate limit will require clever selection and prioritization to target all signal topologies of interest

- The bottomonia and charmonia High Level Triggers are confirmed in the 2022 trigger menu essentially unchanged inspite of the instantaneous luminosity and pileup increase.

Detector, Trigger and Reconstruction Strengths

- Tracking at HLT has changed/evolved from Run 2 to Run 3.
  - For Run 3 the goal is to maintain efficiencies & fake rate levels while reducing the timing & controlling the rate budget.
  - 2018: 3 main global tracking iterations covering from p_T>0.4GeV AND an efficiency recovery iteration at p_T>1.2GeV
  - 2022: One single global iteration covering from p_T>0.3GeV by means of tracks seeded by the Patatrack Pixel Tracks that are obtained exploiting heterogeneous HLT farm (CPU+GPU) [*].
- Specifically for the B-Physics purposes, the GPU pixel tracks are selected in the region around a dimuon candidate. The new displaced charmonium + tracks HLT paths are useful also for spectroscopy studies. Examples:
  - $B_c(2S)$ & $B_c^*(2S)$
  - B_{s2}^* and excited B_s^0 mesons

[*] https://arxiv.org/abs/2008.13461

Prospects for Phase-2 (HL-LHC)

- The data to be collected in Run 3 and Run 4 will help achieve very interesting new results and updated results integrating and/or complementing LHCb results.
  - In Phase-2, the availability of tracking information at Level-1 trigger will be crucial in retaining the full physics potential when pile up conditions increase to <PU>~200.
  - The new MIP Timing Layer (MTD) will allow in Phase-2:
    - Some hadronic PID capabilities for the softer tracks
    - An upgrade of the 3D vertex to a 4D vertex, allowing precision timing for charged hadrons and converted photons and an effective pile up mitigation

Summary

- CMS has proven to be one of the leading experiments in the hadron spectroscopy. The full potentiality of Run 2 is still being explored.

- A lot more to come in Run 3 and the HL-LHC era.

B a c k u p

Expected PID performance

- Expected performance in identifying charged pions, kaons and protons as a function of transverse momentum and rapidity in the barrel and endcap regions of the CMS Phase 2 detector (assuming 30-40 ps time resolution).